Entropy stable high order discontinuous Galerkin methods for ideal compressible MHD on structured meshes

Yong Liu [a], Chi-Wang Shu [b,1], Mengping Zhang [a,*,2]

[a] *School of Mathematical Sciences, University of Science and Technology of China, Hefei, Anhui 230026, PR China*
[b] *Division of Applied Mathematics, Brown University, Providence, RI 02912, USA*

A R T I C L E   I N F O

A B S T R A C T

We present a discontinuous Galerkin (DG) scheme with suitable quadrature rules [15] for ideal compressible magnetohydrodynamic (MHD) equations on structural meshes. The semi-discrete scheme is analyzed to be entropy stable by using the symmetrizable version of the equations as introduced by Godunov [32], the entropy stable DG framework with suitable quadrature rules [15], the entropy conservative flux in [14] inside each cell and the entropy dissipative approximate Godunov type numerical flux at cell interfaces to make the scheme entropy stable. The main difficulty in the generalization of the results in [15] is the appearance of the non-conservative "source terms" added in the modified MHD model introduced by Godunov [32], which do not exist in the general hyperbolic system studied in [15]. Special care must be taken to discretize these "source terms" adequately so that the resulting DG scheme satisfies entropy stability. Total variation diminishing / bounded (TVD/TVB) limiters and bound-preserving limiters are applied to control spurious oscillations. We demonstrate the accuracy and robustness of this new scheme on standard MHD examples.

© 2017 Elsevier Inc. All rights reserved.

1. Introduction

In this paper, we construct an entropy stable discontinuous Galerkin (DG) scheme for the system of ideal compressible magnetohydrodynamic (MHD) equations. As most conservation laws from applications, the entropy condition is an important property for the MHD system. It is highly desirable to design high order DG schemes to satisfy entropy stability. It is well known that a conservation law system has an entropy if and only if it is symmetrizable. Godunov [32] pointed out that systems like MHD which have a divergence constraint cannot be symmetrized unless some additional source terms (which under the divergence-free condition would be zero) are added. Therefore, we will only consider the MHD system with such source terms added.

The ideal MHD equations are a system of conservation laws for the mass, momentum, energy and magnetic field. The magnetic field has to satisfy an extra constraint that its divergence is zero, which is a reflection of the principle that there are no magnetic monopoles. The exact solution of the MHD equations preserves zero divergence for the magnetic field in future time, if the initial divergence is zero. However, in numerical computation, it is not obvious that the divergence

---

free condition will be satisfied. This may lead to instabilities and loss of the positivity for density and pressure in the computations. Many works have dealt with this problem which are based on one dimensional Riemann solvers for the 7×7 system of conservation laws [7,11,12,22]. These schemes add additional steps to take care of the divergence free constraint. In [11] the authors suggest to project the numerical solution to a subspace of zero divergence solutions which involves the solution of an elliptic Poisson equation. Another method is called the constrained transport (CT) by Evans and Hawley [24], which simply means a particular finite difference discretization on a staggered grid which maintains $\nabla \cdot \mathbf{B}$ in a specific discretization. Nonstaggered versions of the CT method have also been developed, see [25,34,47]. Finite volume and discontinuous Galerkin schemes to enforce the exact divergence-free condition are developed in [2,44,4]. Another way to keep the divergence exactly zero is to rewrite the MHD equations in terms of the vector potential $\mathbf{A}$ instead of the magnetic field $\mathbf{B} = \nabla \times \mathbf{A}$. That not only leads to the order of spatial derivatives being increased by one, but also reduces the order of accuracy by one (see [24] for a more in-depth discussion).

A different class of schemes is the 8-wave formulation of the MHD equations suggested by Powell [46], which is found to behave better in terms of stability and accuracy than the discretization of the usual conservative form. Powell noticed that the conservative MHD equations have a Jacobian with a non-physical zero eigenvalue, and the addition of suitable non-conservative source terms would recover the correct physical structure. This approach however leads to a model that is not conservative. According to the Lax–Wendroff theorem [41], however, only conservative schemes can guarantee the correct jump conditions and propagation speed in the limit, for a discontinuous solution [52].

In terms of spatial discretizations, high order schemes have been developed by different techniques, including essentially non-oscillatory (ENO) and weighted ENO (WENO) schemes [39,2], ADER-WENO schemes [5,3], adaptive mesh refinement (AMR) schemes [1], DG schemes with locally or globally divergence-free constraints [43,4], and central DG schemes with arbitrary order exactly divergence-free constraint [44].

The Runge–Kutta discontinuous Galerkin method is a popular category of high order numerical schemes developed in [20,19,18,21]. Jiang and Shu [38] proved a discrete entropy inequality for semi-discrete DG schemes for the square entropy for scalar conservation laws, in arbitrary dimension and on arbitrary triangulations, which is extended to symmetric systems by Hou and Liu [36]. In recent years, entropy stable schemes have been extensively studied. Tadmor [51] established the framework of entropy conservative fluxes and entropy stable fluxes, and Lefloch, Mercier and Rohde [42] provided a procedure to compute high order accurate entropy conservative fluxes. Entropy stable schemes have also been constructed either through the summation-by-parts (SBP) procedure [26,13,29] or through suitable split forms [27,29,30]. Motivated by these approaches, in [15], Chen and Shu discretize the integrals in the DG method by the Gauss–Lobatto type quadratures, resulting in the nodal formulation [35,40], then replace the fluxes inside the cell by entropy conservative fluxes, and take the fluxes across cell interfaces as the usual entropy dissipative fluxes. It is shown in [15] that DG schemes constructed in this general framework satisfy the entropy condition for the given entropy.

The entropy stable schemes have the advantages that the numerical method is nearly isentropic in smooth regions and entropy is guaranteed to be increasing across discontinuities. Thus, the numerics precisely follow the physics of the second law of thermodynamics. Another advantage of entropy stable algorithms is that one can limit the amount of dissipation added to the numerical scheme to guarantee entropy stability. Entropy stable schemes are developed by several authors [8,28,9,10,53,14]. In recent years, especially, the entropy schemes based on finite volume methods are popularly developed. Winters and Gassner [53] designed an affordable analytical expression of the numerical interface flux function that discretely preserves the entropy of the system with a particular source term [37]. Derigs et al. [23] extended this method into multi-physics, multi-scale AMR simulation with high-order in space by using spatial reconstruction techniques. Chandrashekar and Klingenberg [14] constructed the semi-discrete finite volume entropy stable schemes by using the symmetrized version of the equations as introduced by Godunov.

In this paper, we develop a semi-discrete entropy stable DG scheme for the MHD equations, following the approach in [15], on one and two dimensional Cartesian meshes. There is no conceptual difficulty to extend the scheme to three dimensions and to unstructured meshes, again following the framework in [15], however it will become more technical and we leave it for future work. An important ingredient in this general framework is the entropy conservative flux, for which we use the one in [14], originally designed for finite volume schemes. The resulting semi-discrete scheme is proved to be entropy stable, and a fully discrete scheme is obtained by using a Runge–Kutta scheme for time integration. We remark that the appearance of the non-conservative "source terms" added in the modified MHD model introduced by Godunov [32] are necessary in order for the equation to be symmetrizable and to accommodate an entropy inequality on the PDE level. Therefore, in order to establish entropy stability, we develop our scheme based on this non-conservative model, which renders additional technical challenges on the suitable DG discretization for the non-conservative source terms and its compatibility with the entropy stability. It also leaves the possibility as pointed out in [52] that it may give wrong solutions for some discontinuous problems. It will be interesting if it is possible to develop entropy stable schemes using the conservative formulation, which will be left for future investigation.

The organization of the paper is as follows. In section 2, we first recall the ideal MHD equations and its symmetrization properties and Godunov's modification. Then we construct the entropy stable DG scheme for the modified MHD equations in section 3. We provide standard MHD numerical tests in section 4. In section 5 we give a few concluding remarks and perspectives for future work. Finally, in the appendix we provide the proof for the main theorem.

2. Ideal MHD equations

The ideal magneto-hydrodynamical model, or the set of ideal MHD equations, is a system of equations which describes the conservation of mass, momentum, energy, and magnetic field of a particular fluid. This system consists of a set of nonlinear hyperbolic equations,

$$\frac{\partial \rho}{\partial t} + \nabla \cdot (\rho \mathbf{u}) = 0$$

$$\frac{\partial \rho \mathbf{u}}{\partial t} + \nabla \cdot (\rho \mathbf{u}\mathbf{u} + (p + \frac{|\mathbf{B}|^2}{2})I - \mathbf{B}\mathbf{B}) = 0$$

$$\frac{\partial \mathbf{B}}{\partial t} + \nabla \cdot (\mathbf{u}\mathbf{B} - \mathbf{B}\mathbf{u}) = 0$$

$$\frac{\partial E}{\partial t} + \nabla \cdot ((E + p + \frac{|\mathbf{B}|^2}{2})\mathbf{u} - (\mathbf{B} \cdot \mathbf{u})\mathbf{B}) = 0$$

$$(2.1)$$

with the additional divergence constraint

$$\nabla \cdot \mathbf{B} = 0$$

Here ρ is the density, $\mathbf{u}$ is the velocity field, p is the pressure, E is the total energy and $\mathbf{B}$ is the magnetic field. The ratio of the specific heats is given by γ and the total energy E is given by

$$E = \frac{1}{2}\rho |\mathbf{u}|^2 + \frac{1}{2}|\mathbf{B}|^2 + \frac{p}{\gamma - 1}$$

This system combines the equations of gas dynamics with Maxwell equations for problems in which relativistic, viscous, and resistive effects can be neglected; the permeability is set to be unity. If the divergence constraint is satisfied at the initial time, then the equation for $\mathbf{B}$ implies that

$$\frac{\partial}{\partial t}\nabla \cdot \mathbf{B} = 0$$

We rewrite equations (2.1) in conservative form in the two dimensional case

$$\mathbf{w}_t + \nabla \cdot \mathbf{F}(\mathbf{w}) = 0 \tag{2.2}$$

where

$$\mathbf{w} = [\rho, \rho u_x, \rho u_y, \rho u_z, B_x, B_y, B_z, E]^T, \ \mathbf{F}(\mathbf{w}) = [\mathbf{f_1}(\mathbf{w}), \mathbf{f_2}(\mathbf{w})] \tag{2.3}$$

$$\mathbf{f_1} = [\rho u_x, \rho u_x^2 + p + \frac{1}{2}|\mathbf{B}|^2 - B_x^2, \rho u_x u_y - B_x B_y, \rho u_x u_z - B_x B_z, 0, u_x B_y - u_y B_x,$$

$$u_x B_z - u_z B_x, u_x(E + p + \frac{1}{2}|\mathbf{B}|^2) - B_x(u_x B_x + u_y B_y + u_z B_z)]^T \tag{2.4}$$

$$\mathbf{f_2} = [\rho u_y, \rho u_y u_x - B_y B_x, \rho u_y^2 + p + \frac{1}{2}|\mathbf{B}|^2 - B_y^2, \rho u_y u_z - B_y B_z, u_y B_x - u_x B_y, 0,$$

$$u_y B_z - u_z B_y, u_y(E + P + \frac{1}{2}|\mathbf{B}|^2) - B_y(u_x B_x + u_y B_y + u_z B_z)]^T \tag{2.5}$$

2.1. The entropy function for the ideal MHD

It is well known the weak solutions of conservation laws are not unique. If the weak solution satisfies enough entropy conditions, one can obtain uniqueness, at least for the scalar problems [45]. Even if uniqueness may not be guaranteed, it is often also desirable to satisfy an entropy condition in the system case. We recall the definition of an entropy function.

Definition 2.1. A convex function U is called an **entropy** function for the system (2.2) if there exist **entropy fluxes** F_α such that

$$F_\alpha'(\mathbf{w}) = U'(\mathbf{w})\mathbf{f}_\alpha'(\mathbf{w}), \quad \alpha = 1, 2 \tag{2.6}$$

where $U'(\mathbf{w})$ and $F_\alpha'(\mathbf{w})$ are viewed as row vectors, $\mathbf{f}_\alpha'(\mathbf{w})$ is the Jacobian matrix.

The functions (U, F_α) are said to form an entropy pair. If a system of conservation laws have smooth solutions, they satisfy an additional entropy conservation law as can be seen below

$$0 = U'(\mathbf{w})\frac{\partial \mathbf{w}}{\partial t} + U'(\mathbf{w})\mathbf{f}'_\alpha(\mathbf{w})\frac{\partial \mathbf{w}}{\partial x_\alpha} = \frac{\partial U}{\partial t} + \frac{\partial F_\alpha}{x_\alpha} \tag{2.7}$$

where we use the Einstein summation convention on repeated indices like α which runs over the number of spatial dimensions. For solutions which are not smooth, the above equation is replaced with an inequality

$$\frac{\partial U}{\partial t} + \frac{\partial F_\alpha}{\partial x_\alpha} \le 0 \tag{2.8}$$

in the sense of distribution.

Definition 2.2. The conservation law (2.2) is said to be symmetrizable if there exists a change of variables $\mathbf{w} \to \mathbf{v}$ which symmetrizes it, i.e., equation (2.2) becomes

$$\frac{\partial \mathbf{w}}{\partial \mathbf{v}}\frac{\partial \mathbf{v}}{\partial t} + \frac{\partial \mathbf{f}_\alpha}{\partial \mathbf{w}}\frac{\partial \mathbf{w}}{\partial \mathbf{v}}\frac{\partial \mathbf{v}}{\partial x_\alpha} = 0 \tag{2.9}$$

where $\frac{\partial \mathbf{w}}{\partial \mathbf{v}}$ is a symmetric positive definite matrix and $\frac{\partial \mathbf{f}_\alpha}{\partial \mathbf{w}}\frac{\partial \mathbf{w}}{\partial \mathbf{v}}$ are symmetric matrices.

There is a close connection between the existence of an entropy pair and the symmetrization of a system of conservation laws.

Theorem 2.1. *(Mock) A necessary and sufficient condition for the system (2.2) to possess a strictly convex entropy $U(\mathbf{w})$ is that there exists a change of dependent variables $\mathbf{w} = \mathbf{w}(\mathbf{v})$ that symmetrizes (2.2). (For the proof, see, e.g. [31].)*

Now since $\frac{\partial \mathbf{w}}{\partial \mathbf{v}}$ and $\frac{\partial \mathbf{f}_\alpha}{\partial \mathbf{w}}\frac{\partial \mathbf{w}}{\partial \mathbf{v}}$ are both symmetric, there exist functions $\varphi(\mathbf{v})$ and $\psi_\alpha(\mathbf{v})$, called potential function and potential fluxes, such that

$$\varphi'(\mathbf{v}) = \frac{\partial \mathbf{w}}{\partial \mathbf{v}}, \quad \psi'_\alpha(\mathbf{v}) = \mathbf{f}_\alpha(\mathbf{w}(\mathbf{v}))^T \tag{2.10}$$

It is easy to verify that

$$\varphi(\mathbf{v}) = \mathbf{w}^T\mathbf{v} - U, \ \psi_\alpha(\mathbf{v}) = \mathbf{v} \cdot \mathbf{f}_\alpha(\mathbf{w}(\mathbf{v})) - F_\alpha \tag{2.11}$$

For the MHD equations, if we define the thermodynamic entropy [14]

$$s = \ln(p\rho^{-\gamma})$$

then the equations of ideal MHD can be used to derive an equation for ρs

$$\frac{\partial \rho s}{\partial t} + \nabla \cdot (\rho s\mathbf{u}) + (\gamma - 1)\frac{\rho(\mathbf{u} \cdot \mathbf{B})}{p}\nabla \cdot \mathbf{B} = 0$$

Under the constraint $\nabla \cdot \mathbf{B} = 0$, the following quantities

$$U = -\frac{\rho s}{\gamma - 1}, \quad F_\alpha = -\frac{\rho s u_\alpha}{\gamma - 1} \tag{2.12}$$

satisfy an additional conservation law for smooth solutions, so that U is an entropy function. The entropy variables corresponding to the above entropy function are given by

$$\mathbf{v} = U'(\mathbf{w})^T = [\frac{\gamma - s}{\gamma - 1} - \beta|\mathbf{u}|^2, 2\beta\mathbf{u}, 2\beta\mathbf{B}, -2\beta]^T, \ \text{where } \beta = \frac{\rho}{2p}$$

However the change of variable $\mathbf{w} \to \mathbf{v}$ fails to symmetrize the ideal MHD equations [8]. To achieve symmetrization of systems with divergence constraints like the ideal MHD, Godunov [32] introduced a modified form of the ideal MHD equations

$$\frac{\partial \mathbf{w}}{\partial t} + \frac{\partial \mathbf{f}_\alpha}{\partial x_\alpha} + \phi'(\mathbf{v})^T\nabla \cdot \mathbf{B} = 0 \tag{2.13}$$

where

$$\phi(\mathbf{v}) = 2\beta(\mathbf{u} \cdot \mathbf{B}). \tag{2.14}$$

In terms of the components of $\mathbf{v}$, this function can be written as

$$\phi(\mathbf{v}) = -\frac{v_2 v_5 + v_3 v_6 + v_4 v_7}{v_8}$$

which is homogeneous of degree one i.e.

$$\mathbf{v} \cdot \phi'(\mathbf{v})^T = \phi(\mathbf{v}) \tag{2.15}$$

Its Jacobian is given by

$$\phi'(\mathbf{v}) = [0, \mathbf{B}, \mathbf{u}, \mathbf{u} \cdot \mathbf{B}]$$

Since $\nabla \cdot \mathbf{B} = 0$ the above modification is consistent. In these modified equations, the corresponding potential function and potential fluxes are given by

$$\varphi(\mathbf{v}) = \mathbf{w}^T \mathbf{v} - U = \rho + \beta |\mathbf{B}|^2, \tag{2.16}$$

$$\psi_\alpha(\mathbf{v}) = \mathbf{v} \cdot \mathbf{f}_\alpha(\mathbf{w}(\mathbf{v})) + \phi(\mathbf{v}) B_\alpha - F_\alpha = \rho u_\alpha + \beta u_\alpha |\mathbf{B}|^2 \tag{2.17}$$

which satisfy

$$\varphi(\mathbf{v}) = \mathbf{w}^T \mathbf{v} - U, \ \ \psi_\alpha(\mathbf{v}) = \mathbf{v} \cdot \psi'_\alpha(\mathbf{v}) - F_\alpha \tag{2.18}$$

3. Entropy stable high order DG schemes

In this section, we proceed to unravel the entropy stable DG scheme for the modified MHD equations. We firstly consider the one dimensional case. The one-dimensional framework can be directly applied to two-dimensional rectangular meshes through tensor products. We largely follow the approach in [15], paying attention to the complication caused by the non-conservative source terms. The equation we are discretizing is

$$\frac{\partial \mathbf{w}}{\partial t} + \frac{\partial \mathbf{f_1}(\mathbf{w})}{\partial x} + \phi'(\mathbf{v})^T \frac{\partial B_x}{\partial x} = 0 \tag{3.1}$$

Firstly, we assume that we have periodic or compactly supported boundary conditions. Secondly, time is taken to be continuous, so that we conduct semidiscrete analysis. Finally, the numerical solution is assumed to be within the set $\Omega = \{\mathbf{w} \in \mathbb{R}^8 : \rho > 0, \ p > 0\}$.

We firstly construct the DG scheme for equations (3.1). We start from the mesh

$$x_{1/2} < x_{3/2} < \cdots < x_{N+1/2}, \ I_j = [x_{j-1/2}, x_{j+1/2}], \ \Delta x_j = x_{j+1/2} - x_{j-1/2}$$

and the finite element space of polynomial degree k

$$\mathbf{V}_h^k = \left\{ \mathbf{w}_h : \mathbf{w}_h |_{I_j} \in [\mathcal{P}^k(I_j)]^8, 1 \leq j \leq N \right\} \tag{3.2}$$

where $\mathcal{P}^k(I_j)$ is the space of polynomials of degree at most k over the subintervals I_j. Let us define the following notations for the arithmetic average and jump on the interface of any quantity

$$\overline{(\cdot)}_{j+1/2} = \frac{1}{2}[(\cdot)_{j+1/2}^- + (\cdot)_{j+1/2}^+], \quad [\cdot]_{j+1/2} = ((\cdot)_{j+1/2}^+ - (\cdot)_{j+1/2}^-)$$

We find $\mathbf{w}_h \in \mathbf{V}_h^k$, such that for any $\mathbf{v}_h \in \mathbf{V}_h^k$ and $1 \leq j \leq N$

$$\begin{aligned}
\int_{I_j} \frac{\partial \mathbf{w}_h^T}{\partial t} \mathbf{v}_h \, dx = & \int_{I_j} \mathbf{f_1}(\mathbf{w}_h)^T \frac{\partial \mathbf{v}_h}{\partial x} \, dx - \int_{I_j} \phi'(\mathbf{w}_h) \frac{\partial B_x}{\partial x} \mathbf{v}_h \, dx \\
& - \widehat{\mathbf{f_1}}_{j+1/2}^T \mathbf{v}_h(x_{j+1/2}^-) + \widehat{\mathbf{f_1}}_{j-1/2}^T \mathbf{v}_h(x_{j-1/2}^+) \\
& - \frac{1}{2} \phi'(\mathbf{w}_h(x_{j+1/2}^-))[B_x]_{j+1/2} \mathbf{v}_h(x_{j+1/2}^-) \\
& - \frac{1}{2} \phi'(\mathbf{w}_h(x_{j-1/2}^+))[B_x]_{j-1/2} \mathbf{v}_h(x_{j-1/2}^+)
\end{aligned} \tag{3.3}$$

where $\widehat{\mathbf{f_1}}_{j+1/2}$ is a numerical flux at the element interface, depending on the values of numerical solution from both sides

$$\widehat{\mathbf{f_1}}_{j+1/2} = \widehat{\mathbf{f_1}}(\mathbf{w}_h(x_{j+1/2}^-), \mathbf{w}_h(x_{j+1/2}^+)) \tag{3.4}$$

In general, $\widehat{\mathbf{f_1}}_{j+1/2}$ is derived from some (exact or approximate) Riemann solver. Notice that this DG scheme is a combination of the classic DG scheme for conservation laws [19] and the DG method for directly solving the Hamilton–Jacobi equations

[17] in treating the non-conservative terms. Notice also that, in the piecewise constant $k = 0$ case, our DG scheme can be written in the finite volume manner

$$\frac{d}{dt}(\mathbf{w}_h)_j = -\frac{1}{\Delta x_j}(\widehat{\mathbf{f_1}}_{j+1/2} - \widehat{\mathbf{f_1}}_{j-1/2}) - \phi'((\mathbf{w}_h)_j)^T \left(\frac{\overline{(B_x)}_{j+1/2} - \overline{(B_x)}_{j+1/2}}{\Delta x_j}\right) \tag{3.5}$$

which is exactly the same as the finite volume scheme in [14]. Next, we are going to apply the Legendre–Gauss–Lobatto quadrature rule with $k + 1$ quadrature points to approximate the three integrals in (3.3).

3.1. Gauss–Lobatto quadrature and summation-by-parts

Consider the reference element $I = [-1, 1]$ associated with Gauss–Lobatto quadrature points

$$-1 = \xi_0 < \xi_1 < \cdots < \xi_k = 1$$

and quadrature weights $\{\omega_j\}_{j=0}^k$. Define the Lagrangian (nodal) basis polynomials

$$L_j(\xi) = \prod_{\substack{l=0 \\ l \neq j}}^N \frac{\xi - \xi_l}{\xi_j - \xi_l}$$

such that $L_j(\xi_l) = \delta_{jl}$. Let $\langle \cdot, \cdot \rangle$ and $\langle \cdot, \cdot \rangle_\omega$ denote the continuous and discrete inner products

$$\langle u, v \rangle = \int_{-1}^1 uv \, d\xi, \quad \langle u, v \rangle_\omega = \sum_{j=0}^k \omega_j u(\xi_j) v(\xi_j)$$

The difference matrix D is set to be

$$D_{jl} = L_l'(\xi_j) \tag{3.6}$$

and the mass matrix M and stiffness matrix S are defined as

$$M_{jl} = \langle L_j, L_l \rangle_\omega = \omega_j \delta_{jl}, \text{ so that } M = diag\{\omega_0, \cdots, \omega_k\} \tag{3.7}$$

$$S_{jl} = \langle L_j, L_l' \rangle_\omega = \langle L_j, L_l' \rangle \tag{3.8}$$

We first recall the summation-by-parts property [13,15]:

Theorem 3.1. *(Summation-by-parts property). Set the boundary matrix*

$$B = diag\{-1, 0, \cdots, 0, 1\} = diag\{\tau_0, \cdots, \tau_k\} \tag{3.9}$$

Then

$$S = MD, \ MD + D^T M = S + S^T = B \tag{3.10}$$

which is a discrete analogue of integration by parts.

Using the matrices above, we are able to convert (3.3) into a compact matrix vector formulation based on the nodal values. We first introduce some notations

$$x_j(\xi) = \frac{1}{2}(x_{j+1/2} + x_{j-1/2}) + \frac{\xi}{2}\Delta x_j$$

$$B_{x,l} = B_x(x_j(\xi_l)), \ \mathbf{w}_h^l = \mathbf{w}_h(x_j(\xi_l)), \ \mathbf{f_1}^l = \mathbf{f_1}(\mathbf{w}_h^l), \ \phi_l'^T = \phi'(\mathbf{v}(\xi_l))^T, \ l = 0, \cdots k$$

$$\vec{\mathbf{f_1}}_*^{\,j} = [\widehat{\mathbf{f_1}}_{j-1/2}, 0, \cdots, 0, \widehat{\mathbf{f_1}}_{j+1/2}] = [\mathbf{f_1}_*^0, \cdots, \mathbf{f_1}_*^k]$$

$$\vec{\mathbf{g}}^j = [\frac{1}{2}\phi'^T(\mathbf{v})_{j-1/2}^+[B_x]_{j-1/2}, 0, \cdots, 0, -\frac{1}{2}\phi'^T(\mathbf{v})_{j+1/2}^-[B_x]_{j+1/2}] = [\mathbf{g}_0, \cdots, \mathbf{g}_k]$$

We will concentrate on a single element and omit the script j. The entropy stable nodal DG scheme is given by

$$\frac{\Delta x}{2}\frac{d\mathbf{w}_h^p}{dt} + 2\sum_{l=0}^k D_{pl}\mathbf{f_1}_S(\mathbf{w}_h^p, \mathbf{w}_h^l) + \sum_{l=0}^k D_{pl}\phi_p'^T B_{x,l} = \frac{\tau_p}{\omega_p}(\mathbf{f_1}^p - \mathbf{f_1}_*^p) + \frac{\tau_p}{\omega_p}\mathbf{g}_p, \ p = 0, \cdots, k \tag{3.11}$$

where $\mathbf{f_1}_S(\mathbf{w}_h^p, \mathbf{w}_h^l)$ and $\widehat{\mathbf{f_1}}$ are respectively the entropy conservative flux and entropy stable flux proposed by Chandrashekar and Klingenberg [14] and defined as follows:

Definition 3.1. A consistent, symmetric two-point numerical flux $\mathbf{f}_S(\mathbf{u}_L, \mathbf{u}_R)$ is entropy conservative for a given entropy function U if

$$(\mathbf{v}_R - \mathbf{v}_L)^T \mathbf{f}_S(\mathbf{u}_L, \mathbf{u}_R) + (\phi_R - \phi_L)\frac{B_{xR} + B_{xL}}{2} = \psi_R - \psi_L \tag{3.12}$$

where $\mathbf{v}_{L,R}$, $\phi_{R,L}$, $\psi_{R,L}$ and $B_{xR,L}$ are the entropy variables, the function defined in (2.14), potential fluxes $\psi_1(\mathbf{v})$ and magnetic field B_x at the left and right states.

Definition 3.2. A consistent two-point numerical flux $\widehat{\mathbf{f}}(\mathbf{u}_L, \mathbf{u}_R)$ is entropy stable for a given entropy function U if

$$(\mathbf{v}_R - \mathbf{v}_L)^T \widehat{\mathbf{f}}(\mathbf{u}_L, \mathbf{u}_R) + (\phi_R - \phi_L)\frac{B_{xR} + B_{xL}}{2} - (\psi_R - \psi_L) \leq 0 \tag{3.13}$$

The next theorem states that (3.11) is (internally) entropy conservative.

Theorem 3.2. *If $\mathbf{f}_S(\mathbf{u}_R, \mathbf{u}_L)$ is entropy conservative in the sense of (3.12), then (3.11) is also conservative within a single element, i.e. it satisfies*

$$\frac{d}{dt}\left(\sum_{p=0}^{k} \frac{\Delta x}{2}\omega_p U_p\right) = \mathcal{F}_k - \mathcal{F}_0 \tag{3.14}$$

where

$$\mathcal{F}_k = (\psi_k - \mathbf{v}_k^T \mathbf{f_1}_*^k) - \phi_k \overline{(B_x)}_k \tag{3.15}$$

$$\mathcal{F}_0 = (\psi_0 - \mathbf{v}_0^T \mathbf{f_1}_*^0) - \phi_0 \overline{(B_x)}_0. \tag{3.16}$$

Moreover, the scheme is at least k-th order accurate measured by local truncation errors.

Proof. The proof of this theorem is provided in the Appendix A. □

For the MHD equations, Chandrashekar and Klingengberg [14] suggested the following entropy conservative flux

$$f_{1S}^{(1)} = \hat{\rho}\bar{u}_x$$

$$f_{1S}^{(2)} = \frac{\bar{\rho}}{2\bar{\beta}} + \bar{u}_x f_{1S}^{(1)} + \frac{1}{2}\overline{|\mathbf{B}|^2} - \bar{B}_x \bar{B}_x$$

$$f_{1S}^{(3)} = \bar{u}_y f_{1S}^{(1)} - \bar{B}_x \bar{B}_y$$

$$f_{1S}^{(4)} = \bar{u}_z f_{1S}^{(1)} - \bar{B}_x \bar{B}_z$$

$$f_{1S}^{(5)} = 0$$

$$f_{1S}^{(6)} = \frac{1}{\bar{\beta}}(\overline{\beta u_x}\bar{B}_y - \overline{\beta u_y}\bar{B}_x)$$

$$f_{1S}^{(7)} = \frac{1}{\bar{\beta}}(\overline{\beta u_x}\bar{B}_z - \overline{\beta u_z}\bar{B}_x)$$

$$f_{1S}^{(8)} = \frac{1}{2}\left[\frac{1}{(\gamma-1)\hat{\beta}} - \overline{|\mathbf{u}|^2}\right]f_{1S}^{(1)} + \bar{u}_x f_{1S}^{(2)} + \bar{u}_y f_{1S}^{(3)} + \bar{u}_z f_{1S}^{(4)}$$

$$\qquad + \bar{B}_x f_{1S}^{(5)} + \bar{B}_y f_{1S}^{(7)} + \bar{B}_z f_{1S}^{(7)} - \frac{1}{2}\bar{u}_x\overline{|\mathbf{B}|^2} + (\bar{u}_x\bar{B}_x + \bar{u}_y\bar{B}_y + \bar{u}_z\bar{B}_z)\bar{B}_x$$

where $\hat{(\cdot)}$ is logarithmic average of two strictly positive quantities as

$$\hat{\alpha} = \frac{\alpha_r - \alpha_l}{\ln\alpha_r - \ln\alpha_l}$$

The next theorem establishes that entropy stable interface numerical fluxes make the whole scheme entropy stable.

Theorem 3.3. *If the numerical flux $\widehat{\mathbf{f}}_1$ at the element interface is entropy stable, then the scheme (3.11) is entropy stable.*

Proof. According to (3.14), the entropy production rate at the interface is

$$(\psi_k^j - (\mathbf{v}_k^j)^T \widehat{\mathbf{f_1}}_{j+1/2}) - \phi_k^j \overline{(B_x)}_k^j - (\psi_0^{j+1} - (\mathbf{v}_0^{j+1})^T \widehat{\mathbf{f_1}}_{j+1/2}) + \phi_0^{j+1} \overline{(B_x)}_0^{j+1}$$

$$= (\mathbf{v}_0^{j+1} - \mathbf{v}_k^j)^T \widehat{\mathbf{f_1}}_{j+1/2}(\mathbf{w}_h^{k,j}, \mathbf{w}_h^{0,j+1}) - (\psi_0^{j+1} - \psi_k^j) + \frac{(B_x)_{j+1/2}^- + (B_x)_{j+1/2}^+}{2}(\phi_0^{j+1} - \phi_k^j)$$

which is non-positive as $\widehat{\mathbf{f_1}}$ is entropy stable. By the assumption of periodic or compactly supported boundary condition, the whole scheme is entropy stable. $\square$

As we know, for systems, most popular numerical fluxes rely on exact or approximate Riemann solver. The Godunov flux based on exact Riemann solvers is by definition entropy stable. Many approximate Riemann solvers, such as the *HLL* or Lax–Friedrichs fluxes are also entropy stable provided the left and right wave speeds λ_L and λ_R are properly chosen [10]. We will use the Lax–Friedrichs fluxes in our computation in next section. When strong shocks appear, limiters such as the TVD/TVB limiter [49,20] and/or the bound-preserving limiter [54] as an extra stabilizing mechanism help to reduce numerical oscillation. Fortunately, the bound-preserving limiter does not increase entropy, and the TVD/TVB limiter also does not increase entropy when applied componentwise [15].

4. Numerical examples

In this section, we present numerical examples on standard one and two dimensional MHD test cases to illustrate the accuracy and robustness of the entropy stable DG scheme in computing smooth and discontinuous flows. The semi-discrete scheme (3.11) is integrated in time using the classical third order accurate strong stability preserving Runge–Kutta scheme [50,33]. We compute on elements of degree $k = 2$ and set the CFL number to be 0.15 for all experiments. The time step is chosen based on the following CFL condition

$$\Delta t = cfl \cdot \min_j \left(\frac{|(\bar{u}_x)_j| + (c_{f,x})_j}{\Delta x} \right)^{-1} \quad \text{for the one dimensional case} \tag{4.1}$$

$$\Delta t = cfl \cdot \min_{i,j} \left(\frac{|(\bar{u}_x)_{i,j}| + (c_{f,x})_{i,j}}{\Delta x} + \frac{|(\bar{u}_y)_{i,j}| + (c_{f,y})_{i,j}}{\Delta y} \right)^{-1} \quad \text{for the two dimensional case} \tag{4.2}$$

where $c_{f,x}$ and $c_{f,y}$ are the fast speeds in the x and y directions, see [39] for the definition.

4.1. One dimensional Riemann problems

In this section, we solve standard one-dimensional Riemann problems. The initial condition for the first Riemann problem is given by

$$(\rho, u_x, u_y, u_z, B_y, B_z, p) = \begin{cases} (1.000, 0, 0, 0, +1, 0, 1.0) \text{ for } x < 0 \\ (0.125, 0, 0, 0, -1, 0, 0.1) \text{ for } x > 0 \end{cases} \tag{4.3}$$

with $B_x = 0.75$ and $\gamma = 2$ on the computational domain $[-1, 1]$. This is the example used by Brio and Wu in [12] to show the formation of the compound wave in MHD.

The solution at $t = 0.2$ is shown in Fig. 4.1, which includes the left moving waves: the fast rarefaction wave, the intermediate shock attached by a slow rarefaction wave; and the right moving waves: the contact discontinuity, a slow shock, and a fast rarefaction wave. The results obtained with 5000 cells serve as reference in Fig. 4.1. We can see that all the waves are resolved well with 800 cells.

The initial condition for the second Riemann problem is

$$(\rho, u_x, u_y, u_z, B_y, B_z, p) = \begin{cases} (1.000, 0, 0, 0, +1, 0, 1000) \text{ for } x < 0 \\ (0.125, 0, 0, 0, -1, 0, 0.10) \text{ for } x > 0 \end{cases} \tag{4.4}$$

with $B_x = 0$ and $\gamma = 2$. This problem is used to evaluate the code for high Mach number flow. The computational domain is taken to be $[-1, 1]$. The solution at $t = 0.012$ is shown in Fig. 4.2. Again, the resolution is good with 200 cells.

In both problems we have applied the TVB limiter with the TVB constant $M = 10$ in the local characteristic fields computed by the eigenvectors evaluated with the cell averages, see [15] for the details of the implementation of such limiters. We remark that the application of the TVB limiter in the local characteristic fields would not guarantee the entropy non-increasing property. In some of the later examples, we plot the evolution of entropy to indicate that it is still numerically decaying with time with a fully discretized scheme and with the TVB limiter applied in the local characteristic fields.
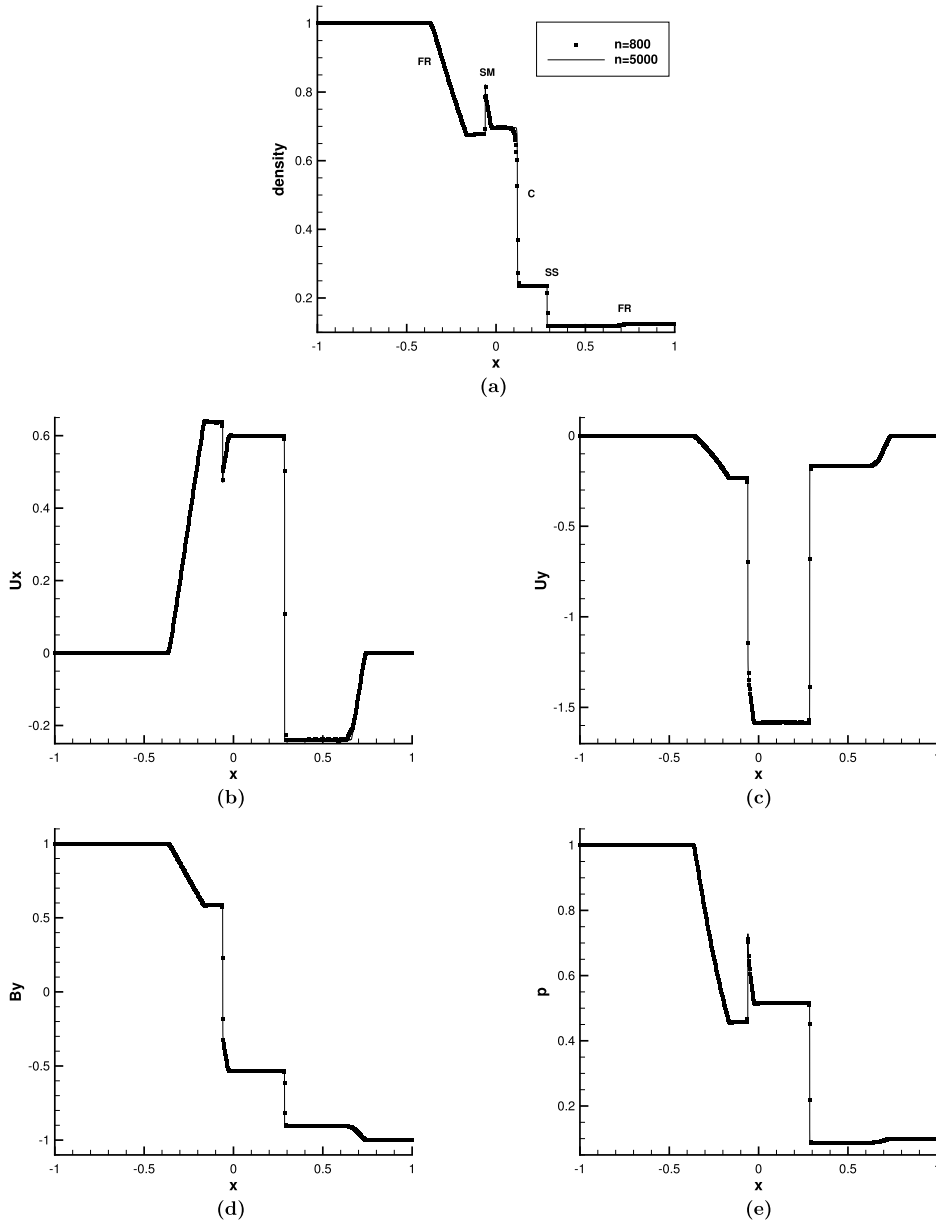
Fig. 4.1. The first one-dimensional Riemann example with 800 cells (squares) on a background solid line computed with 5000 cells. $t = 0.2$ and $M = 10$. The symbol FR denotes a fast rarefaction wave; SM is a compound wave (an intermediate shock followed by a slow rarefaction wave); C is a contact discontinuity; SS is a slow shock. Top: ρ; middle left: u_x; middle right: u_y; bottom left: B_y; bottom right: p.

4.2. The torsional Alfvén wave pulse

Next we consider the propagation of a torsional Alfvén wave pulse [6] which is initialized as

$$(\rho, u_x, B_x, p) = (1, 10, 10/\sqrt{4\pi}, 0.01),$$

$$(u_x, u_y) = 10(\cos\phi, \sin\phi), \ (B_y, B_z) = -10(\cos\phi, \sin\phi),$$

with a pulse around the center of the computational domain $[-0.5, 0.5]$. Here $\phi = \frac{\pi}{8}(\tanh(\frac{0.25+x}{\delta}) + 1)(\tanh(\frac{0.25-x}{\delta}) + 1)$ with $\delta = 0.005$. The boundary conditions are periodic and $\gamma = 5/3$. In this example, the initial pressure is very small, which is less than ten-thousandth of the total energy. It is easy for most numerical schemes to produce negative pressure, hence we use the positive-preserving limiter [16]. The scheme is carried out on a uniform mesh with $N = 800$ cells. In Fig. 4.3, we present the total energy and pressure at $t = 0.156$. Note that there are two pulses in the solution, and successful simulation should properly preserve the shape of these features.
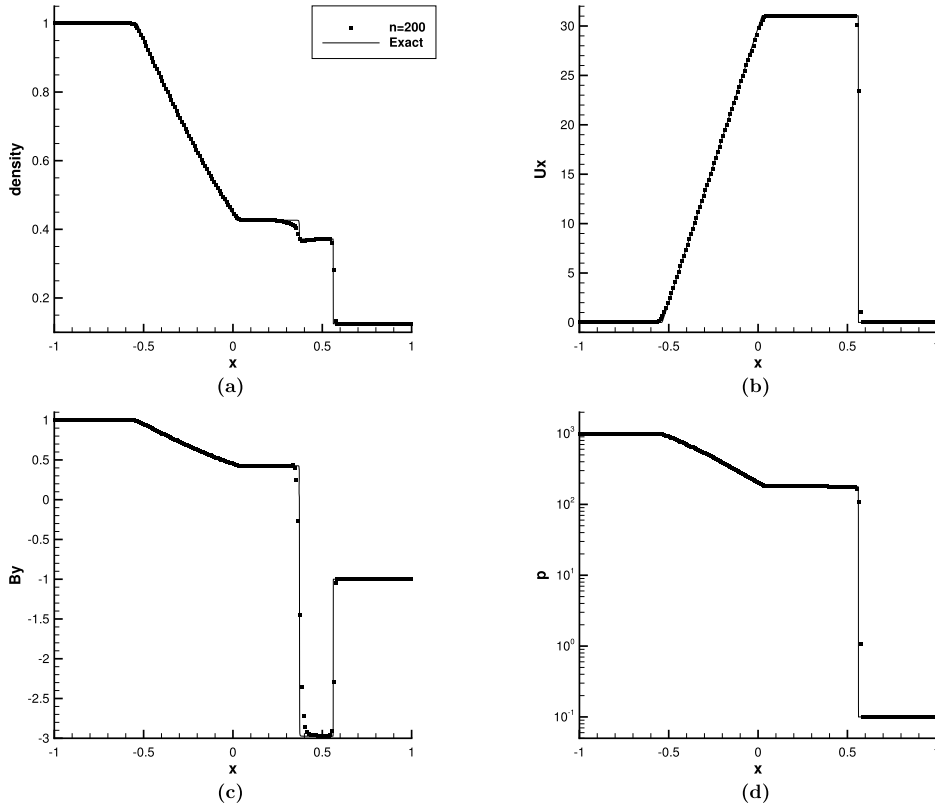
Fig. 4.2. The second one-dimensional Riemann example with 200 cells (squares) on a background solid line of the exact solution. $t = 0.012$ and $M = 10$. Top left: ρ; top right: u_x; bottom left: B_y; bottom right: p.
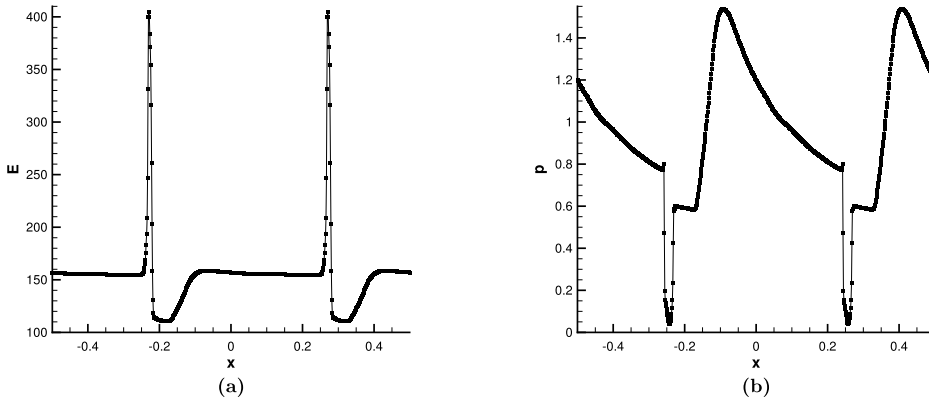

Fig. 4.3. The total energy E (left) and pressure p (right) of the torsional Alfvén wave pulse on an 800 cell mesh at $t = 0.156$.

4.3. The Orszag–Tang vortex problem

In this subsection, we consider the Orszag–Tang vortex problem which is a widely used test example in MHD simulations. The initial conditions are taken as in [14]

$$\rho = \frac{25}{36\pi}, \ \mathbf{u} = (-\sin(2\pi y), \sin(2\pi x), 0), \ p = \frac{5}{12\pi},$$

$$\mathbf{B} = \frac{1}{\sqrt{4\pi}}(-\sin(2\pi y), \sin(4\pi x), 0)$$

The computational domain is taken to be $[0, 1] \times [0, 1]$ with periodic boundary conditions on all sides, the constant $\gamma = 5/3$. The smooth initial conditions evolve into a more complex flow with many discontinuities. We use uniform meshes to
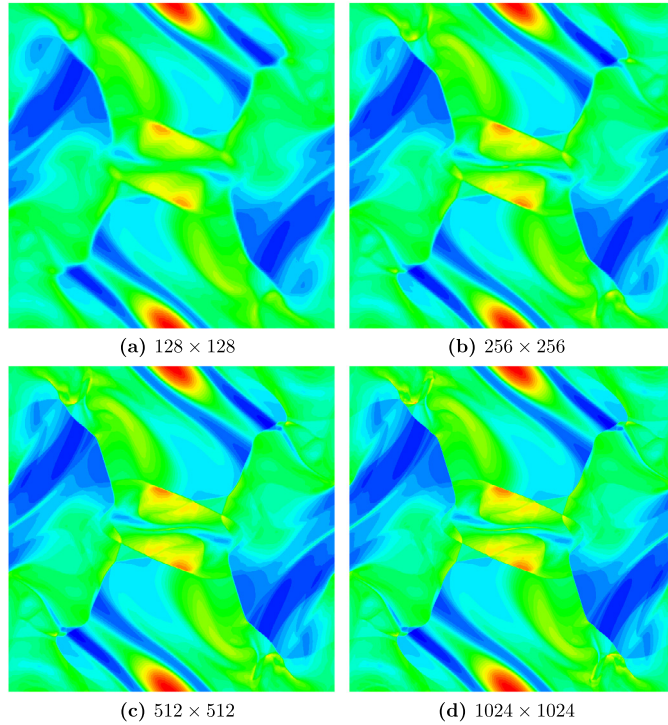
(a) 128×128 **(b)** 256×256

(c) 512×512 **(d)** 1024×1024

Fig. 4.4. Density at $t = 0.5$ for the Orszag–Tang test case on different meshes. The density range is 0.09 to 0.48.
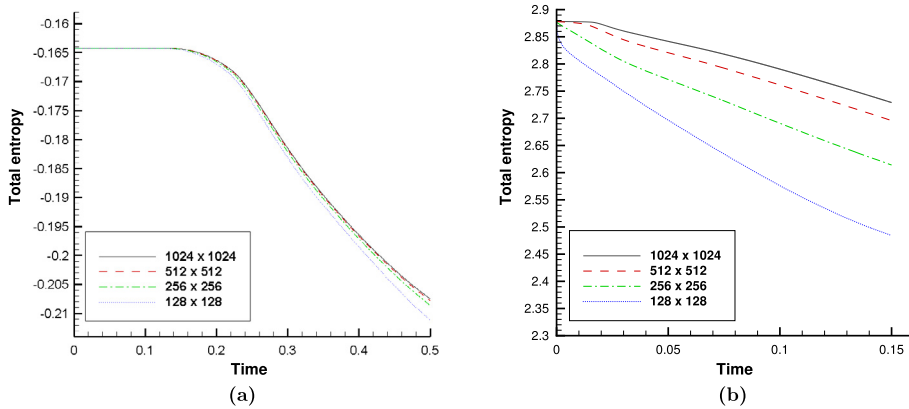

Fig. 4.5. Evolution of the total entropy with time for the (a) Orszag–Tang test (b) rotor test.

implement the scheme. The solution at $t = 0.5$ is shown in Fig. 4.4 on meshes of sizes 128×128, 256×256, 512×512 and 1024×1024 with $M = 10$. We find that the scheme is stable on all the meshes, including on the very fine mesh, which shows the robustness of the scheme. With explicit time discretization by a Runge–Kutta scheme, we cannot prove the entropy stability, hence we compute the total entropy $\sum_{i,j} \sum_{p=0}^{k} \omega_p U((\mathbf{w}_h^{p,n})_{i,j}) \Delta x \Delta y$ which in principle should decrease with time if the scheme is entropy stable. Fig. 4.5a shows that this quantity does not increase with time during the simulation.

4.4. The rotor test

This test case was first proposed in [7] but we use the version given in [52], where it is referred to as the *first rotor problem*. The computational domain is $[0, 1] \times [0, 1]$ with periodic boundary conditions on all sides, the constant $\gamma = 1.4$ and initial condition is given as follows
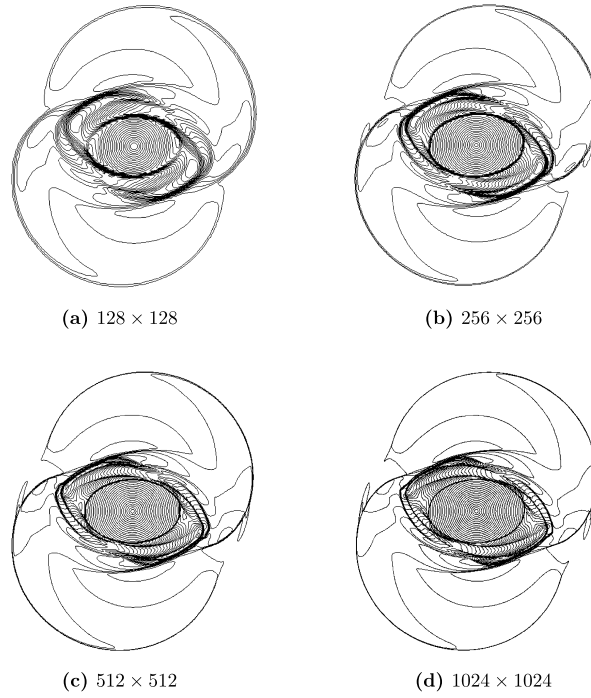
(a) 128×128 (b) 256×256

(c) 512×512 (d) 1024×1024

Fig. 4.6. Mach contours for the rotor test case at time $t = 0.15$ on different meshes. 30 contours between 0 and 4.2 are shown.

$$(\rho, u_x, u_y) = \begin{cases} (10, \dfrac{u_0}{r_0}(-(y-1/2)), \dfrac{u_0}{r_0}(x-1/2)) \text{ for } r < r_0 \\[2mm] (1+9f, \dfrac{fu_0}{r}(-(y-1/2)), \dfrac{fu_0}{r}(x-1/2)), \ f = \dfrac{r_1 - r}{r_1 - r_0} \text{ for } r_0 \leq r < r_1 \\[2mm] (1,0,0) \text{ for } r_1 \leq r \end{cases} \tag{4.5}$$

where $r = \sqrt{(x-1/2)^2 + (y-1/2)^2}$, $r_1 = 0.1$, $r_0 = 0.115$ and $u_0 = 2$. The rest of the quantities are constants and are given by

$$u_z = 0, \ p = 1.0, \ \mathbf{B} = \frac{5}{\sqrt{4\pi}}(1,0,0)$$

The results at $t = 0.15$ are obtained on meshes with 128×128, 256×256, 512×512 and 1024×1024 cells with $M = 10$. The contours of the Mach number $\mathbf{u}/c_s$ with the sound speed $c_s = \sqrt{\gamma p/\rho}$ are shown in Fig. 4.6. Similarly to what the authors of [7] and [52] have noted, when using the standard DG method, some "distortion" around the central rotating area can be observed [43]. There is no distortion in Fig. 4.6 for our entropy stable DG scheme, and also we have the positivity of the density and pressure without using the bound-preserving limiter for this example. The total entropy is shown in Fig. 4.5b, and we again observe a monotonic decay which indicates that the fully discrete scheme is also entropy stable.

4.5. Smooth Alfvén waves

This test is taken from [52] and consists of a circularly polarized Alfvén wave which propagates at an angle of $\alpha = 30°$. The computational domain is taken to be $[0, 1/\cos\alpha] \times [0, 1/\sin\alpha]$ with periodic boundary conditions. The constant $\gamma = 5/3$ and the initial condition is given as follows

$$\rho = 1, \ (u_x, u_y) = v_\perp(-\sin\alpha, \cos\alpha), \ p = 0.1$$

$$B_x = B_\parallel \cos\alpha - B_\perp \sin\alpha, \ B_y = B_\parallel \sin\alpha + B_\perp \cos\alpha, \ B_z = u_z = 0.1\cos(2\pi x_\parallel)$$

$$B_\parallel = 1, \ B_\perp = v_\perp = 0.1\sin(2\pi x_\parallel), \ x_\parallel = x\cos\alpha + y\sin\alpha$$

The solution have periodicity, it returns to its initial state after a time of $t = 1$ units which is the period of the solution. We show errors in the L^1 and L^2 norms of $B_\perp$ in Table 4.1 at time $t = 5$. We can see that the optimal order of error accuracy is obtained.

Table 4.1
L^1 and L^2 errors of $B_\perp$ and corresponding convergence rates for the circularly polarized Alfvén wave at $t = 5$.

N×N	L^1-error	Order	L^2-error	Order
32×32	3.48E−05	–	2.61E−05	–
64×64	3.71E−06	3.23	2.71E−06	3.27
128×128	4.25E−07	3.12	3.11E−07	3.13
256×256	4.98E−08	3.10	3.90E−08	2.99

(a) ρ

(b) p

(c) $u_\parallel$

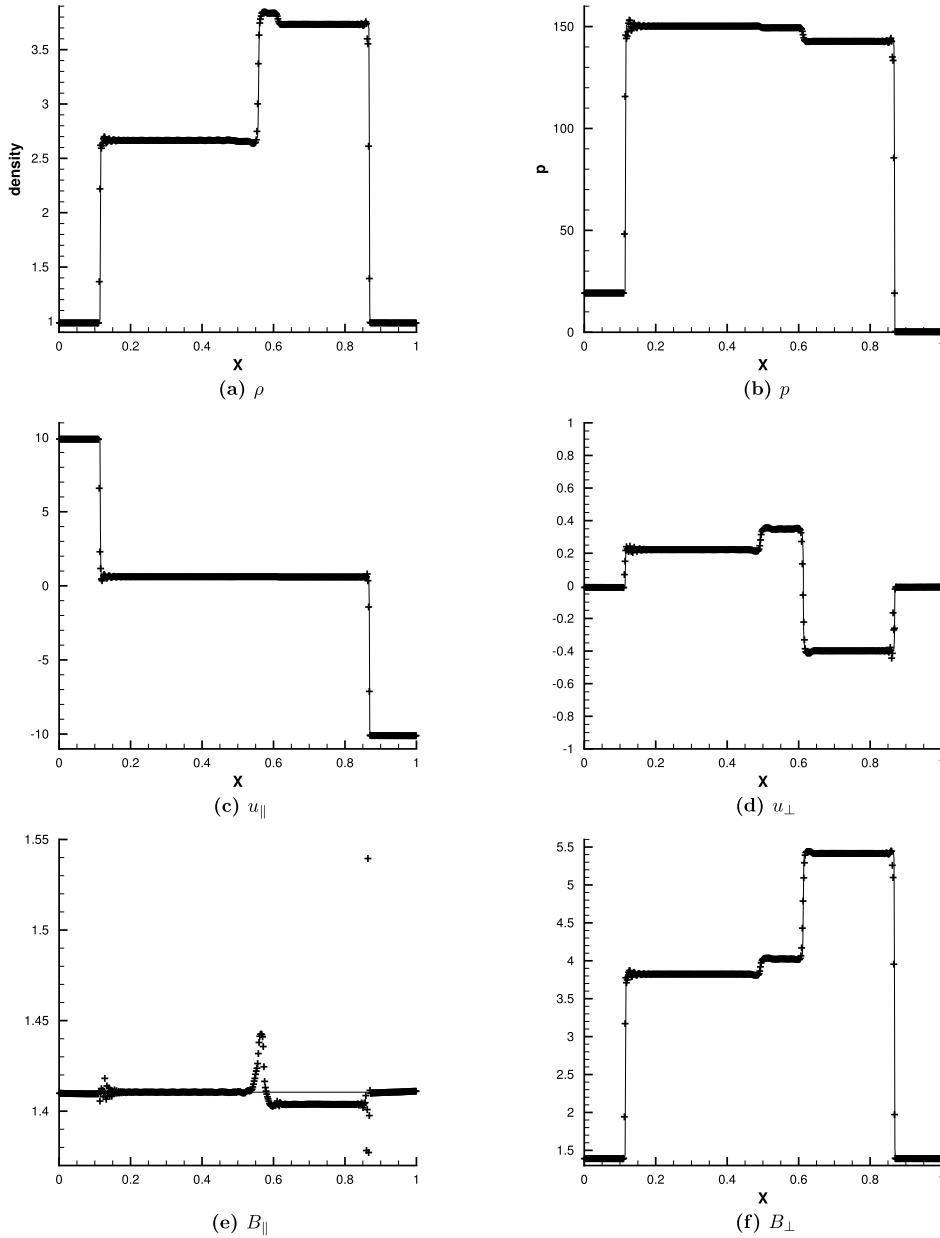(d) $u_\perp$

(e) $B_\parallel$

(f) $B_\perp$

Fig. 4.7. The solution of the $2D$ rotated shock tube problem by the entropy stable DG scheme (symbols) on a mesh with 512×2 cells. For comparison, the non-rotated $1D$ solution with 800 cells is also plotted (solid line).

4.6. Rotated shock tube problem

This test case is taken from [48] and the shock propagates at an angle of $\alpha = 45°$. The initial left state is $(\rho, u_\parallel, u_\perp, u_z, B_\parallel, B_\perp, B_z, p) = (1, 10, 0, 0, 5/\sqrt{4\pi}, 5/\sqrt{4\pi}, 0, 20)$ and the initial right state is $(1, -10, 0, 0, 5/\sqrt{4\pi}, 5/\sqrt{4\pi}, 0, 1)$.

The mesh is Cartesian with $\Delta x = \Delta y$; we use 2 cells in the y direction and 512 cells in the x direction. The left and right boundaries are fixed according to the initial condition since the computation is stopped at time $t = 0.08 \cos \alpha = 0.08/\sqrt{2}$ before the fast shocks would reach the left and right boundaries. The top and bottom boundaries are of the shifted periodic type according to the translational symmetry in the $(-1, 1)$ direction as explained in [52]. We plot the first row ($j = 1$) of the physical mesh in Fig. 4.7. This may be compared with the solution from [48] except that they plot the slice along the line $x = y$. We also have the problem that the parallel component of the magnetic field $B_\parallel$, which should be constant, shows a large error due to the non-conservative formulation, similar to the results in [52] from a non-conservative 8-wave scheme. The other quantities have good behavior in comparison with the results in [48].

5. Concluding remarks

We have constructed a DG scheme for the symmetrizable ideal compressible magnetohydrodynamic equations with non-conservative source terms. Thanks to the general framework established in [15], the entropy conservative numerical flux [14] used inside the cell, and the entropy dissipative Godunov type numerical flux used at the cell interfaces, this scheme can be proved to be entropy stable in the semi-discrete case when the additional non-conservative source terms are discretized carefully. Limiters including the bound-preserving limiter and the TVD/TVB limiter are applied in test cases with strong shocks. We have provided numerical results for standard MHD test cases to show the accuracy and robustness of the scheme in computing smooth and discontinuous solutions. The additional non-conservative source terms introduced by Godunov are necessary to obtain a symmetrizable formulation and an entropy condition. There is still a conflict between the entropy stability which requires the non-conservative source terms, and the conservation property which is lost due to these source terms, as mentioned in [14]. In future work, we will extend the method to 3D and to unstructured meshes, which involves heavier technicality but no conceptual difficulty due to the general framework in [15]. We would also like to construct entropy stable DG schemes in the conserved formulation of MHD, but this would need new ideas if we do not want to adopt globally divergence-free bases, which seem unnatural for DG schemes.

Appendix A. Proof of Theorem 3.2

Proof. Entropy conservation:

$$
\frac{d}{dt}\left(\sum_{p=0}^{k} \frac{\Delta_x}{2} \omega_p U_p \right) = \sum_{p=0}^{k} \frac{\Delta_x}{2} \omega_p \mathbf{v}_p^T \frac{d\mathbf{w}_h^p}{dt}
$$

$$
= \sum_{p=0}^{k} \tau_p \mathbf{v}_p^T (\mathbf{f_1}^p - \mathbf{f_1}_*^p) + \sum_{p=0}^{k} \tau_p \mathbf{v}_p^T \mathbf{g}_p
$$

$$
- 2 \sum_{p=0}^{k} \sum_{l=0}^{k} S_{pl} \mathbf{v}_p^T \mathbf{f_1}_S(\mathbf{w}_h^p, \mathbf{w}_h^l) - \sum_{p=0}^{k} \sum_{l=0}^{k} S_{pl} \phi_p B_{x,l}
$$

here, we have used the fact that $\phi(\mathbf{v})$ is homogeneous of degree one (2.15). Using the SBP property the third term is

$$
\sum_{p=0}^{k} \sum_{l=0}^{k} (B_{pl} + S_{pl} - S_{lp}) \mathbf{v}_p^T \mathbf{f_1}_S(\mathbf{w}_h^p, \mathbf{w}_h^l) = \sum_{p=0}^{k} \tau_p \mathbf{v}_p^T \mathbf{f_1}^p + \sum_{p=0}^{k} \sum_{l=0}^{k} S_{pl} (\mathbf{v}_p - \mathbf{v}_l)^T \mathbf{f_1}_S(\mathbf{w}_h^p, \mathbf{w}_h^l)
$$

$$
= \sum_{p=0}^{k} \tau_p \mathbf{v}_p^T \mathbf{f_1}^p + \sum_{p=0}^{k} \sum_{l=0}^{k} S_{pl} (\psi_p - \psi_l) - \sum_{p=0}^{k} \sum_{l=0}^{k} S_{pl} \left(\frac{B_{x,p} + B_{x,l}}{2} \right) (\phi_p - \phi_l)
$$

$$
= \sum_{p=0}^{k} \tau_p (\mathbf{v}_p^T \mathbf{f_1}^p - \psi_p) - \sum_{p=0}^{k} \sum_{l=0}^{k} S_{pl} \left(\frac{B_{x,p} + B_{x,l}}{2} \right) (\phi_p - \phi_l)
$$

Then

$$
\frac{d}{dt}\left(\sum_{p=0}^{k} \frac{\Delta_x}{2} \omega_p U_p \right) = \sum_{p=0}^{k} \tau_p (\psi_p - \mathbf{v}_p^T \mathbf{f_1}_*^p) + \sum_{p=0}^{k} \sum_{l=0}^{k} S_{pl} \left(\frac{B_{x,p} + B_{x,l}}{2} \right) (\phi_p - \phi_l)
$$

$$
- \sum_{p=0}^{k} \sum_{l=0}^{k} S_{pl} \phi_p B_{x,l} + \sum_{p=0}^{k} \tau_p \mathbf{v}_p^T \mathbf{g}_p
$$

The second term is

$$\sum_{p=0}^{k}\sum_{l=0}^{k}\frac{1}{2}S_{pl}(\phi_p B_{x,p}+\phi_p B_{x,l}-\phi_l B_{x,p}-\phi_l B_{x,l})$$

$$=\frac{1}{2}\sum_{p=0}^{k}\sum_{l=0}^{k}(\phi_p(S_{pl}-S_{lp})B_{x,l})-\frac{1}{2}\sum_{l=0}^{k}\tau_l\phi_l B_{x,l}$$

$$=\frac{1}{2}\sum_{p=0}^{k}\sum_{l=0}^{k}(\phi_p(S_{pl}+S_{pl}-B_{pl})B_{x,l})-\frac{1}{2}\sum_{l=0}^{k}\tau_l\phi_l B_{x,l}$$

$$=\sum_{p=0}^{k}\sum_{l=0}^{k}\phi_p S_{pl}B_{x,l}-\sum_{l=0}^{k}\tau_l\phi_l B_{x,l}$$

Hence

$$\frac{d}{dt}\left(\sum_{p=0}^{k}\frac{\Delta_x}{2}\omega_p U_p\right)=\sum_{p=0}^{k}\tau_p(\psi_p-\mathbf{v}_p^T\mathbf{f1}_*^p)+\sum_{p=0}^{k}\tau_p\mathbf{v}_p^T\mathbf{g}_p-\sum_{l=0}^{k}\tau_l\phi_l B_{x,l}$$

$$=(\psi_k-\mathbf{v}_k^T\mathbf{f1}_*^k)-(\psi_0-\mathbf{v}_0^T\mathbf{f1}_*^0)-\frac{1}{2}\phi_k[B_x]_k-\frac{1}{2}\phi_0[B_x]_0-\phi_k B_{x,k}+\phi_0 B_{x,0}$$

$$=(\psi_k-\mathbf{v}_k^T\mathbf{f1}_*^k)-(\psi_0-\mathbf{v}_0^T\mathbf{f1}_*^0)-\phi_k\overline{(B_x)}_k+\phi_0\overline{(B_x)}_0$$

$$=\mathcal{F}_k-\mathcal{F}_0$$

Accuracy: Since the difference matrix D is exact for polynomials of degree up to k, and the entropy conservative flux is symmetric and consistent, the truncation error is $\mathcal{O}(\Delta x^k)$ and the scheme is at least k-th order accurate when polynomials of degree k is used. See [15] for more details. As we can see from the numerical examples, the scheme gives the optimal $(k+1)$-th order accuracy for our smooth solution test case. □

References

[1] D.S. Balsara, Divergence-free adaptive mesh refinement for magnetohydrodynamics, J. Comput. Phys. 174 (2001) 614–648.
[2] D.S. Balsara, Divergence-free reconstruction of magnetic fields and WENO schemes for magnetohydrodynamics, J. Comput. Phys. 228 (2009) 5040–5056.
[3] D.S. Balsara, M. Dumbser, Divergence-free MHD on unstructured meshes using high order finite volume schemes based on multidimensional Riemann solvers, J. Comput. Phys. 299 (2015) 687–715.
[4] D.S. Balsara, R. Käppeli, Von Neumann stability analysis of globally divergence-free RKDG schemes for the induction equation using multidimensional Riemann solvers, J. Comput. Phys. 336 (2017) 104–127.
[5] D.S. Balsara, T. Rumpf, M. Dumbser, C.D. Munz, Efficient, high accuracy ADER-WENO schemes for hydrodynamics and divergence-free magnetohydrodynamics, J. Comput. Phys. 228 (2009) 2480–2516.
[6] D.S. Balsara, D. Spicer, Maintaining pressure positivity in magnetohydrodynamic simulations, J. Comput. Phys. 148 (1999) 111–148.
[7] D.S. Balsara, D. Spicer, A staggered mesh algorithm using high order Godunov fluxes to ensure solenoidal magnetic fields in magnetohydrodynamic simulations, J. Comput. Phys. 149 (1999) 270–292.
[8] T. Barth, Numerical methods for gasdynamic systems on unstructured grids, in: Kroner, Ohlberger, Rohde (Eds.), An Introduction to Recent Developments in Theory and Numerics for Conservation Laws, in: Lecture Notes in Computational Science and Engineering, vol. 5, Springer-Verlag, 1998, pp. 198–285.
[9] T. Barth, On the role of involutions in the discontinuous Galerkin discretization of Maxwell and magnetohydrodynamic systems, in: Compatible Spatial Discretizations, Springer, New York, 2006, pp. 69–88.
[10] F. Bouchut, C. Klingenberg, K. Waagan, A multiwave approximate Riemann solver for ideal MHD based on relaxation. I: theoretical framework, Numer. Math. 108 (2007) 7–42.
[11] F. Brackbill, D. Barnes, The effect of nonzero $\nabla\cdot\mathbf{B}$ on the numerical solution of the magnetohydrodynamic equations, J. Comput. Phys. 35 (1988) 426–430.
[12] M. Brio, C.C. Wu, An upwind differencing scheme for the equations of ideal magnetohydrodynamics, J. Comput. Phys. 75 (1988) 400–422.
[13] M.H. Carpenter, T.C. Fisher, E.J. Nielsen, S.H. Frankel, Entropy stable spectral collocation schemes for the Navier–Stokes equations: discontinuous interfaces, SIAM J. Sci. Comput. 36 (2014) B835–B867.
[14] P. Chandrashekar, C. Klingenberg, Entropy stable finite volume scheme for ideal compressible MHD on 2-D Cartesian meshes, SIAM J. Numer. Anal. 54 (2016) 1313–1340.
[15] T. Chen, C.-W. Shu, Entropy stable high order discontinuous Galerkin methods with suitable quadrature rules for hyperbolic conservation laws, J. Comput. Phys. 345 (2017) 427–461.
[16] Y. Cheng, F. Li, J. Qiu, L. Xu, Positivity-preserving DG and central DG methods for ideal MHD equations, J. Comput. Phys. 238 (2013) 255–280.
[17] Y. Cheng, C.-W. Shu, A discontinuous Galerkin finite element method for directly solving the Hamilton–Jacobi equations, J. Comput. Phys. 223 (2007) 398–415.
[18] B. Cockburn, S. Hou, C.-W. Shu, The Runge–Kutta local projection discontinuous Galerkin finite element method for conservation laws IV: the multidimensional case, Math. Comput. 54 (1990) 545–581.
[19] B. Cockburn, S.-Y. Lin, C.-W. Shu, TVB Runge–Kutta local projection discontinuous Galerkin finite element method for conservation laws III: one-dimensional systems, J. Comput. Phys. 84 (1989) 90–113.
[20] B. Cockburn, C.-W. Shu, TVB Runge–Kutta local projection discontinuous Galerkin finite element method for conservation laws II: general framework, Math. Comput. 52 (1989) 411–435.

[21] B. Cockburn, C.-W. Shu, The Runge–Kutta discontinuous Galerkin method for conservation laws V: multidimensional systems, J. Comput. Phys. 141 (1998) 199–224.
[22] W. Dai, P.R. Woodward, An approximate Riemann solver for ideal magnetohydrodynamics, J. Comput. Phys. 111 (1994) 354–372.
[23] D. Derigs, A.R. Winters, G.J. Gassner, S. Walch, A novel high-order, entropy stable, 3D AMR MHD solver with guaranteed positive pressure, J. Comput. Phys. 317 (2016) 233–256.
[24] C.R. Evans, J.F. Hawley, Simulation of magnetohydrodynamic flows – a constrained transport method, Astrophys. J. 332 (1988) 659–677.
[25] M. Fey, M. Torrilhon, A constrained transport upwind scheme for divergence-free advection, in: Hyperbolic Problems: Theory, Numerics, Applications, Springer, Berlin, Heidelberg, 2003, pp. 529–538.
[26] T.C. Fisher, M.H. Carpenter, High-order entropy stable finite difference schemes for nonlinear conservation laws: finite domains, J. Comput. Phys. 252 (2013) 518–557.
[27] T.C. Fisher, M.H. Carpenter, J. Nordström, N.K. Yamaleev, C. Swanson, Discretely conservative finite-difference formulations for nonlinear conservation laws in split form: theory and boundary conditions, J. Comput. Phys. 234 (2013) 353–375.
[28] G. Gallice, Positive and entropy stable Godunov-type schemes for gas dynamics and MHD equations in Lagrangian or Eulerian coordinates, Numer. Math. 94 (2003) 673–713.
[29] G.J. Gassner, A skew-symmetric discontinuous Galerkin spectral element discretization and its relation to SBP-SAT finite difference methods, SIAM J. Sci. Comput. 35 (2013) A1233–A1253.
[30] G.J. Gassner, A.R. Winters, D.A. Kopriva, A well balanced and entropy conservative discontinuous Galerkin spectral element method for the shallow water equations, Appl. Math. Comput. 272 (2016) 291–308.
[31] E. Godlewski, P. Raviart, Numerical Approximation of Hyperbolic Systems of Conservation Laws, Springer, 1996.
[32] S.K. Godunov, The symmetric form of magnetohydrodynamics equations, in: Numerical Methods for Mechanics of Continuum Medium, vol. 1, 1972, pp. 26–34.
[33] S. Gottlieb, C.-W. Shu, E. Tadmor, Strong stability-preserving high-order time discretization methods, SIAM Rev. 43 (2001) 89–112.
[34] C. Helzel, J.A. Rossmanith, B. Taetz, An unstaggered constrained transport method for the 3D ideal magnetohydrodynamic equations, J. Comput. Phys. 230 (2011) 3803–3829.
[35] J.S. Hesthaven, T. Warburton, Nodal Discontinuous Galerkin Methods: Algorithms, Analysis, and Applications, Springer Science & Business Media, 2007.
[36] S. Hou, X.-D. liu, Solutions of multi-dimensional hyperbolic systems of conservation laws by square entropy condition satisfying discontinuous Galerkin method, J. Sci. Comput. 31 (2007) 127–151.
[37] P. Janhunen, A positive conservative method for magnetohydrodynamics based on HLL and Roe methods, J. Comput. Phys. 160 (2000) 649–661.
[38] G.S. Jiang, C.-W. Shu, On a cell entropy inequality for discontinuous Galerkin methods, Math. Comput. 62 (1994) 531–538.
[39] G.S. Jiang, C.C. Wu, A high-order WENO finite difference scheme for the equations of ideal magnetohydrodynamics, J. Comput. Phys. 150 (1999) 561–594.
[40] D.A. Kopriva, G. Gassner, On the quadrature and weak form choices in collocation type discontinuous Galerkin spectral element methods, J. Sci. Comput. 44 (2010) 136–155.
[41] P. Lax, B. Wendroff, Systems of conservation laws, Commun. Pure Appl. Math. 13 (1960) 217–237.
[42] P.G. Lefloch, J.-M. Mercier, C. Rohde, Fully discrete, entropy conservative schemes of arbitrary order, SIAM J. Numer. Anal. 40 (2002) 1968–1992.
[43] F. Li, C.-W. Shu, Locally divergence-free discontinuous Galerkin methods for MHD equations, J. Sci. Comput. 22 (2005) 413–442.
[44] F. Li, L. Xu, Arbitrary order exactly divergence-free central discontinuous Galerkin methods for ideal MHD equations, J. Comput. Phys. 231 (2012) 2655–2675.
[45] E. Lodlewski, P.-A. Raviart, Hyperbolic Systems of Conservation Laws, Ellipses, 1991.
[46] K.G. Powell, An approximate Riemann solver for magnetohydrodynamics, in: Upwind and High-Resolution Schemes, Springer, Berlin, Heidelberg, 1997, pp. 570–583.
[47] J.A. Rossmanith, An unstaggered, high-resolution constrained transport method for magnetohydrodynamic flows, SIAM J. Sci. Comput. 28 (2006) 1766–1797.
[48] D. Ryu, F. Miniati, T.W. Jones, A. Frank, A divergence-free upwind code for multidimensional magnetohydrodynamic flows, Astrophys. J. 509 (1998) 244.
[49] C.-W. Shu, TVB uniformly high-order schemes for conservation laws, Math. Comput. 49 (1987) 105–121.
[50] C.-W. Shu, S. Osher, Efficient implementation of essentially non-oscillatory shock-capturing schemes, J. Comput. Phys. 77 (1988) 439–471.
[51] E. Tadmor, The numerical viscosity of entropy stable schemes for systems of conservation laws, Math. Comput. 49 (1987) 91–103.
[52] G. Tóth, The $\nabla \cdot \mathbf{B} = 0$ constraint in shock-capturing magnetohydrodynamics codes, J. Comput. Phys. 161 (2000) 605–652.
[53] A.R. Winters, G.J. Gassner, Affordable, entropy conserving and entropy stable flux functions for the ideal MHD equations, J. Comput. Phys. 304 (2016) 72–108.
[54] X. Zhang, C.-W. Shu, On positivity-preserving high order discontinuous Galerkin schemes for compressible Euler equations on rectangular meshes, J. Comput. Phys. 229 (2010) 8918–8934.